

# Supporting Information:

## Free energy analysis along the stalk mechanism of membrane fusion

Shuhei Kawamoto<sup>1</sup> and Wataru Shinoda<sup>1</sup>

<sup>1</sup>Health Research Institute, National Institute of Advanced Industrial Science & Technology  
(AIST), 1-8-31, Midorigaoka, Ikeda, Osaka 563-8577, Japan

### 1. Choice of the parameters for the guiding potentials

Here, we give here variables  $p(\lambda) = \{R_1, R_2, z_1, z_2, z_3\}$  as functions of a control parameter,  $\lambda$ , and four parameters,  $a_1$ ,  $a_2$ ,  $a_3$ , and  $a_4$ , to guide the membrane morphology from the two apposed membranes to the stalk formation and the fusion pore.

$$R_1 = \max\{-a_4, (-a_1 + a_2)/2 + (\lambda - 1/2)(a_1 + a_2)\} \quad (\text{S1})$$

$$R_2 = \max\{a_3, a_3 + (2\lambda - 1)(a_2 - a_3)\} \quad (\text{S2})$$

$$z_1 = \max\{a_4, z_2\} \quad (\text{S3})$$

$$z_2 = \max\{a_1 - \lambda(a_1 + a_2), -a_3\} \quad (\text{S4})$$

$$z_3 = z_2 + a_3 + \min\{a_1, 2\lambda a_1\} \quad (\text{S5})$$

Figure 2c in the main text plots the variables with the parameters:  $a_1=2.0$  nm,  $a_2=4.0$  nm,  $a_3=1.0$  nm, and  $a_4=0.5$  nm.

The parameters,  $a_1$  and  $a_2$ , determine the initial membrane distance ( $=2a_1$ ) and the final fusion pore radius, respectively. These values are chosen to be large enough to cover the equilibrium of the membrane distance and the fusion pore radius within a sampling range of  $0 \leq \lambda \leq 1$ . Thus, the state at  $\lambda = 0$  does not correspond to the minimum energy of the separated

membranes. The state at  $\lambda = 1$  is not also the minimum energy, either. However, we found the local energy minima in the range of  $0 \leq \lambda \leq 1$ .

The parameter  $a_3$  is the initial radius of the cylindrical guiding potential. We have to choose the appropriate radius  $a_3$  to guide the membrane morphology towards the stalk formation and to calculate the free energy properly. If a radius  $a_3 \leq 0.5$  nm is chosen, we cannot guide the membranes to form a stable stalk. Even at  $a_3 = 0.5$  nm, the two flat membranes were connected only by a single alkyl-chain of the lipid tail, in a pre-stalk configuration (Fig. S1), and it did not grow to a stable stalk in the limited simulation time. A radius of  $a_3 \geq 1.2$  nm, on the other hand, is obviously too large: it exceeds the optimal stalk radius. This results in an overestimation of the free energy associated with the stalk formation. With a proper choice of  $a_3$  in a range of  $0.6 \leq a_3 \leq 1.0$  nm, the guiding potential leads the system to a reasonable stalk formation with the concomitant expected morphological changes of the membranes. The free energy of the stalk with respect to the separated membranes ( $\Delta G_{\text{stalk}} = \Delta G(\lambda=0.5) - \Delta G(\lambda=0.12)$ ) is plotted as a function of the radius  $a_3$ . There is a plateau on the free energy profile in the range  $0.6 \leq a_3 \leq 1.0$  nm, within an error of  $1 k_B T$ .

The parameter  $a_4$  determines the final ring-height of the type A potential ( $= 2a_4$ ). We also checked the effect of the parameter  $a_4$  on the evaluated free energy value. A choice in the range of  $0.3 \leq a_4 \leq 1.0$  nm is useful to steer the membrane morphology to open a fusion pore and gives the minimum free energy.

We also check the effect of apex angle of the guiding cylinder on the calculated free energy. Fig. S2 shows the free energy of the stalk with respect to two separated membranes. It clearly demonstrates that the shape of the cylinder top does not affect the calculated free energy value. The reason why we chose the pointing cylinder instead of flat top is to control the local membrane interface continuously when the cylinder converts into the ring along the control parameter  $\lambda$ . (See Fig. 2(b))

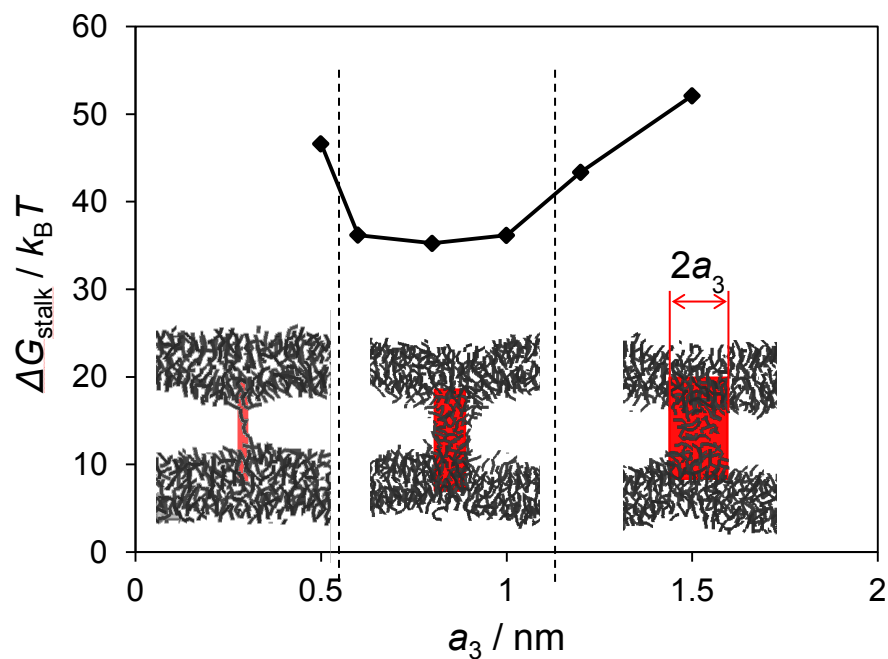


FIG. S1. Free energy of the stalk with respect to the two separated membranes,  $\Delta G_{\text{stalk}}$ , as a function of the cylinder radius  $a_3$  of the guiding potential. Snapshots are sequentially taken from the simulations with  $a_3 = 0.5, 1.0,$  and  $1.5$  nm, from left to right. The lipid alkyl chains are shown as black lines and the cylindrical guiding potential is shown in red.

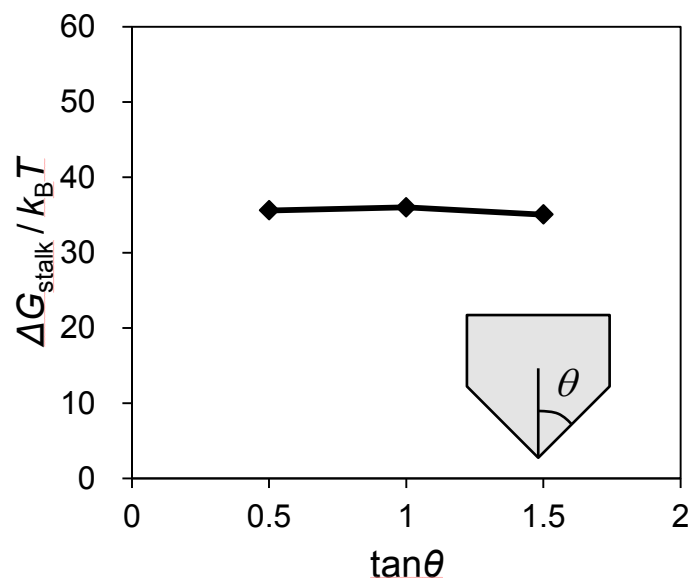


FIG. S2. Free energy of stalk with respect to two separated membranes,  $\Delta G_{\text{stalk}}$ , as a function of apex angle of the cylinder top of the guiding potential.

## 2. Relaxation MD from the transition states

Figure 3S shows a comparison of density maps of lipid tail and headgroup between the guided MD simulation and non-guided MD simulations starting from the transition states. We have repeatedly carried out the latter MD runs from several different configurations, and typical relaxation processes are shown in the Figure. It is clear that, in the relaxation process from the transition state, the system follows the very similar pathway as guided by the guiding potential used for the free energy computation. The speed of the relaxation is different in each relaxation MD runs, though the observed relaxation process seems to take place along the same (or very similar) pathway. This may suggest that the guiding method successfully guides the membranes along the minimum energy pathway.

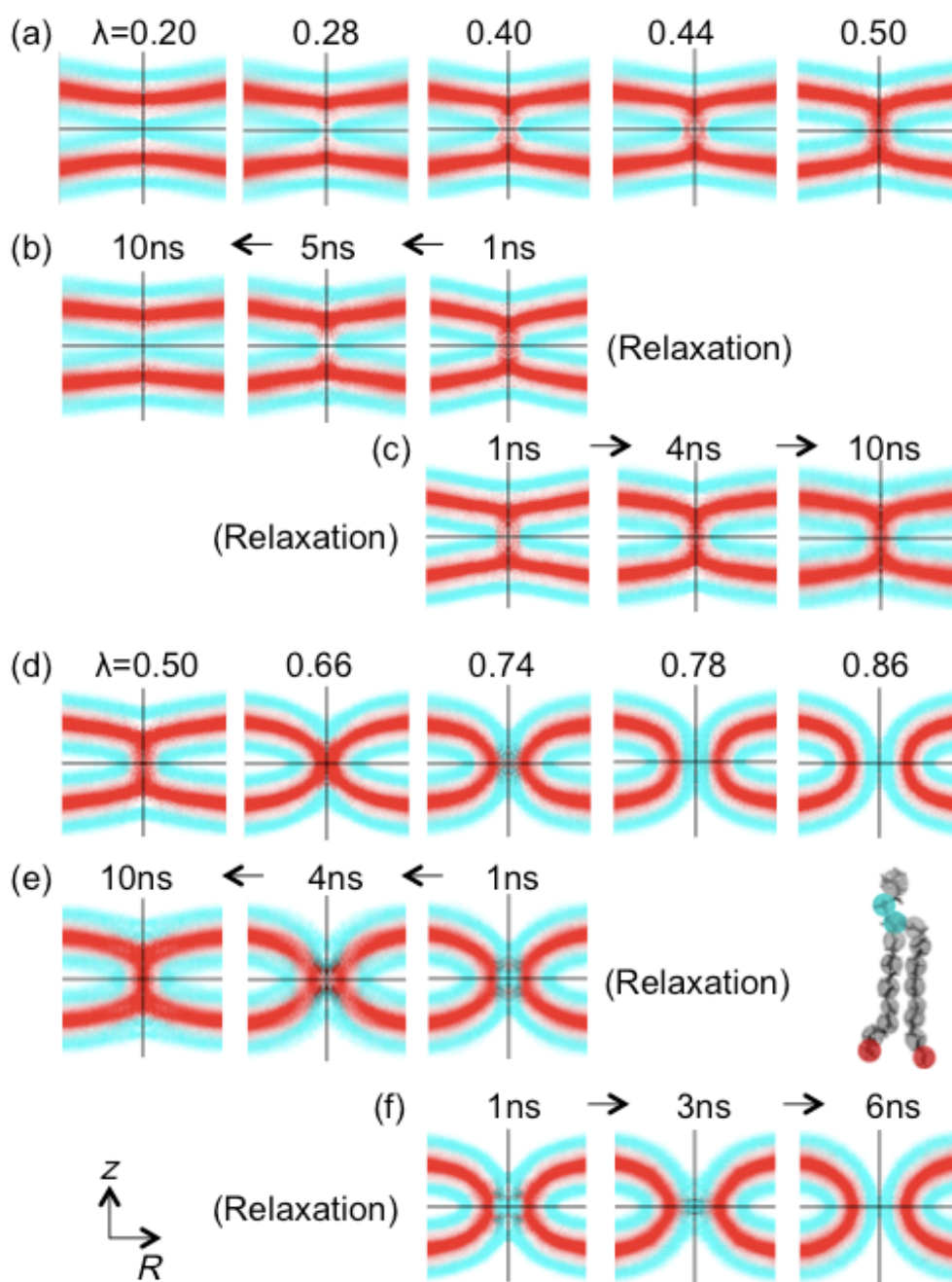


Fig. S3 Density distribution of lipid tail and headgroup particles in the guided fusion process and relaxation MD simulation from the transition states. (a) and (d) show the density in the guided MD simulation. (b) and (c) show a density map in a relaxation process from the transition state of pre-stalk formation (backward and forward processes, respectively). (e) and (f) show a density map in a relaxation process from the transition state of pre-pore formation. Color code is the same as in Fig. 6 in the main text.